TWO-DIMENSIONAL COMPUTATIONAL ANALYSIS OF 'HIGH TAIL' CONFIGURATION AIRCRAFT WAKE VORTEX PAIRS

Chris L. ELLIS, **Kris RYAN and Gregory J. SHEARD**

Fluids Laboratory for Aeronautical and Industrial Research (FLAIR), Department of Mechanical and Aerospace Engineering, Monash University, VIC 3800, Australia

ABSTRACT

This paper investigates how the two-dimensional kinematics differs in the wake vortices from a 'high tail' aircraft compared with a conventional 'flat tail' configuration. While analytical methods can be used to construct a description of such vortex pairs, this research utilizes a more realistic vortex profile, allowing the viscous effect on the interaction to be captured. The flow is modeled in a two-dimensional plane, with the vortex pairs positioned as if the plane was located a short distance downstream of the aircraft. To model the 'high tail' wing / tail configuration, the inner vortex pair is initially positioned above the centerline of the vortex pair produced by the aircraft wings. The simulation is integrated forward in time to capture the motion and interaction of the counter-rotating vortex pairs for comparison against a reference case where the two sets of vortex pairs are initially aligned horizontally. Computations employed a spectral-element discretization in space, and a third-order backwards multistep method for time integration. Variation of the vertical positioning of the two sets of counter-rotating vortex pairs was found to alter the two-dimensional kinematics caused by the viscous interaction of the vortex pairs. This paper describes these interactions.

NOMENCLATURE

b_0	Span of aircraft wing
b_1	Span of wing vortex pair
b_2	Span of tail vortex pair.
C_L	Lift coefficient
AR	Wing aspect ratio
Γ_1	Circulation of wing vortex
Γ_2	Circulation of tail vortex
Re	Reynolds number
υ	Kinematic viscosity
r	Vortex radius
ρ	Incompressible fluid density
p	Kinematic static pressure
g	Gravity acceleration vector
$\mathbf{u}$	Two-dimensional velocity vector field
u	Velocity in the x direction
t	Time
t_0	Period of one rotation of the tail vortex pair
$\bar{t}$	Non-dimensional time
Z	Downstream distance
h	Vertical displacement of tail vortex pair
L^2	L^2 norm across the domain
m	Number of side elements within the central resolved domain
n	Polynomial degree in spectral elements
r_0	Vortex core radius
ε	Percentage deviation in L^2 from highest n

INTRODUCTION

Wake vortices are a byproduct of lift on the wings of an aircraft. They are produced when the high pressure air from underneath the wing flows around the outer edges of the wing tip. This causes a vortex structure to form behind the aircraft (McCormick BW, 1995). These vortices have the effect of creating a net downward flow behind the aircraft, countering the lift of any aircraft that is trailing the lead aircraft. They can pose a real danger to following aircraft, as evidenced by the crash of an American Airlines Airbus A300 in New York, on 12 November 2001, due to a failure of its rudder when abrupt corrections were applied after passing through another aircraft's wake (NTSB Report Number AAR-04-04).

As aircraft are becoming larger and larger, the wake vortices they produce are also increasing in size and strength. This is limits the maximum passenger throughput of airports, and therefore motivates research into mechanisms for reducing the impact of these vortices in aviation.

Simple vortex pairs have been investigated since the 1970s (Barker and Crow, 1977). More recently, it has been shown that the strength of the vortex pair produced from the tail of an aircraft can be anywhere up to 50% of the strength of the vortex pair produced by the wings (Rennich and Lele, 1999). The presence of the vortex pair shed by the tail can have a significant effect on the two dimensional kinematic properties of the stronger vortex pair shed by the wings. While this has been investigated by Fabre et al (2002), and Crouch (1997) the focus has been on potential ways to force three-dimensional instabilities to form in the main wing vortex pair. To date, no research has investigated how a change

in the aircraft tail configuration affects the overall vortex system. For such aircraft as the C-17 Globemaster heavy lift aircraft, the tail can be displaced up to 20% of the span of the wings.

This research is particularly pertinent to military airfields where the majority of the aircraft are either very large, heavy lift aircraft, such as the C-17, or much smaller fighter type aircraft.

This research is a beginning into an extensive investigation into the effect of a 'high tail' aircraft configuration on its wake vortex system. While this study only investigates the wing/tail configuration in two-dimensions, future work will extend to three-dimensional instability and vortex interaction.

MODEL DESCRIPTION
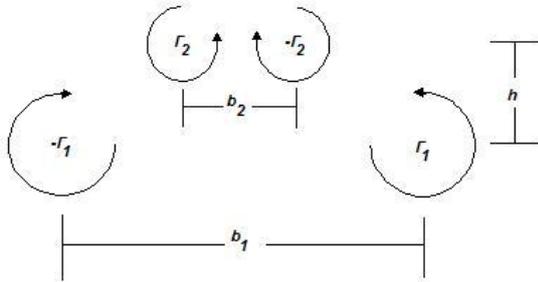
Figure 1: Diagram displaying the layout of the initial vortex set and defining the span and height variables.

It can be seen in Figure 1 the geometry and circulation of the wing/tail vortex set and the variables that are defined in the next section. The setup of the wing/tail vortex set is two pairs of counter-rotating vortex pairs with the tail vortex pair in opposition to the wing vortex pair.

The problem is simulated using the incompressible two-dimensional Navier Stokes equation,

$$\frac{\partial \mathbf{u}}{\partial t} = -(\mathbf{u} \cdot \nabla)\mathbf{u} - \nabla p + \upsilon \nabla^2 \mathbf{u}, \tag{1}$$

and the continuity equation,

$$\nabla \cdot \mathbf{u} = 0. \tag{2}$$

The vortex profile used is that of a Gaussian vortex profile,

$$\upsilon = \frac{\Gamma}{2\pi r}\left(1 - e^{-\left(\frac{r}{r_0}\right)^2}\right). \tag{3}$$

In this case, Re is defined based on the circulation of the wing vortex, Γ_1, and the kinematic viscosity, υ, as

$$Re = \frac{\Gamma_1}{\upsilon}. \tag{4}$$

For these simulations the Re was set at 20,030 to be consistent with the ranges used in similar vortex studies (Roy et al 2008).

The problem is related back to real conditions through the non-dimensional time as defined by Fabre et al (2002),

$$\bar{t} = \frac{\Gamma_1}{2\pi b_0^2}(t - t_0). \tag{5}$$

By taking the ratio of $\frac{b_1}{b_0} = \frac{\pi}{4}$ from Donaldson and Bilanin (1975) for an elliptically loaded wing the value of b_0 can be found and related to the downstream distance Z as defined by Fabre et al (2002),

$$\frac{Z}{b_0} = \frac{4\pi AR}{C_L}\left(1 + \frac{\Gamma_2 b_2}{\Gamma_1 b_1}\right)\left(\frac{b_1}{b_0}\right)^3 \bar{t}. \tag{6}$$

By substituting all of the values in, it is found that 100 time units corresponds to a value of $\bar{t} = 4.3985$ and $\frac{Z}{b_0} = 143.95$. Relating this back to the span of the original aircraft, the downstream distance of 7.448 km corresponds to 100 time units and 104.6 seconds for an aircraft travelling at a landing speed of 70 m/s.

The problem was computed using an in-house code employing a spectral-element discretization in space and a third-order backwards multistep scheme for time integration. The solver employs a nodal formulation, in which Lagrangian tensor-product polynomials are employed in each element. The degree of this polynomial, *n*, can be changed for a given simulation to control special resolution. More information on this method can be seen in Karniadakis et al (1991).

The mesh used is shown in Figure 2 and is sufficiently large to cause the boundary effects in the less-resolved region to become negligible. On the mesh boundaries, a Dirichlet condition is imposed on the velocity field as a cross flow to prevent the vortex system from migrating from the refined region of the mesh. As the outer region contains no important flow structures, it is less resolved to reduce the computational expense of the simulations. Despite the initial configuration possessing a reflective symmetry about the vertical centerline, the full system of vortices was resolved and evolved to permit two-dimensional, symmetry-breaking behavior in the evolving vortices to be captured.
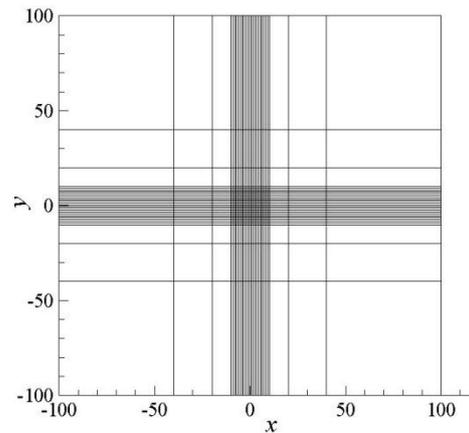
Figure 2: Plot showing mesh in two dimensions with a finely resolved section from $x = -10,10$ and $y = -10,10$. The finely resolved section is a box with *m* x *m* elements.

Initial conditions

Figure 3(a) shows the control case of the 'flat tail' configuration with $h = 0$. A value of $\frac{\Gamma_2}{\Gamma_1} = 0.4$ was chosen for the ratio between the wing and tail circulation and this corresponds to the values found in the literature for a heavy life aircraft in landing configuration (Rennich and Lele, 1999). The horizontal displacement of the tail to wing separation was chosen to be $\frac{b_2}{b_1} = 0.38$ and this corresponds to the geometry of the C-17 Globemaster aircraft.

(a)

(b)
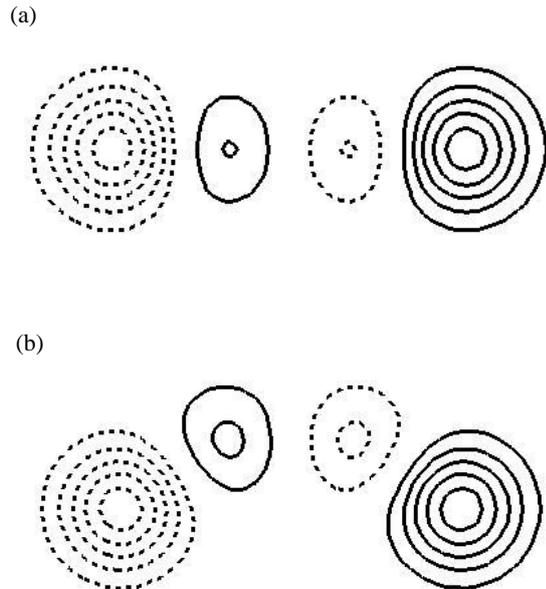
Figure 3: (a) Contour plot of initial vorticity for the flat tail case in two-dimensional space. **(b)** Contour plot of initial vorticity for the high tail case in two-dimensional space. Each contour line represents a vorticity scale of 1. Minimum vorticity is -5.6 with a maximum of 5.6 in the left and right wing vortex respectively. Dashed lines represent negative vorticity.

Figure 3(b) displays the initial position of the 'high tail' case and the only change from the 'flat tail' case is the vertical displacement of the tail vortex pair. The ratio of $\frac{h}{b_1} = 0.2$ was chosen to correspond to the vertical displacement of the tail of the C-17 Globemaster aircraft from its wings.

Error analysis

The simulation errors were approximated by taking L^2 which is defined as,

$$L^2 \equiv \oint_\Omega |u| d\Omega. \qquad (7)$$

Because of the lack of fluid flow outside of the central resolved region, the large size of the domain did not have a major effect on the accuracy of the L^2. To analyze the convergence the order of the polynomial interpolation was increased for a single simulation initial condition. As can be seen in Figure 4, the percentage difference in the L^2 between the case of $n = 20$ and $n = 11$ is only 0.9%. This shows that the simulations are showing good convergence for the $n = 13$ case which was used for the simulations.
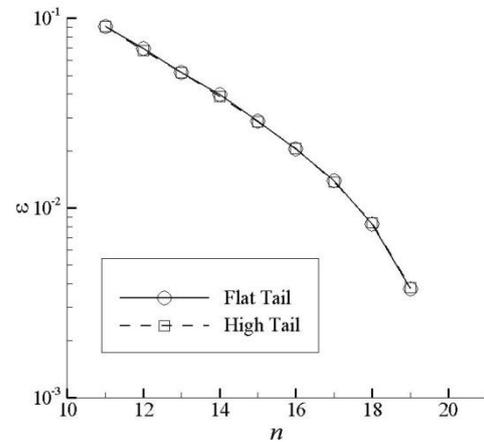
Figure 4: Plot of the percentage difference in L^2 norm with respect to a solution with $n = 20$ (ε) against element of polynomial degree n. ○ represents the flat tail case and □ represents the high tail case. The data was taken at 10 time units.

RESULTS

Wake kinematics

Initially, a small change in the height of the tail can have a significant effect on the movement of the vortex pair produced by the main wing.

Figure 5 shows the small amount that the wing vortex pair from the 'flat tail' configuration descends during the 10 time units. It also displays how the tail vortex pair becomes elongated and reduced in size during its transit around the wing vortex pair.

Figure 6 shows how the tail vortex pair descends considerably faster in the 'high tail' configuration during the 10 time units. In this configuration, the tail vortex pair retains most of its size and shape and doesn't exhibit the elongation that's present in the 'flat tail' configuration.

As can be seen in Figure 7 (a), the 'flat tail' case, the wing vortex pair only travels to a vertical displacement of approximately $0.4b_1$ from an initial position of 0 over 10 time units.

3

(a)

(b)

(c)
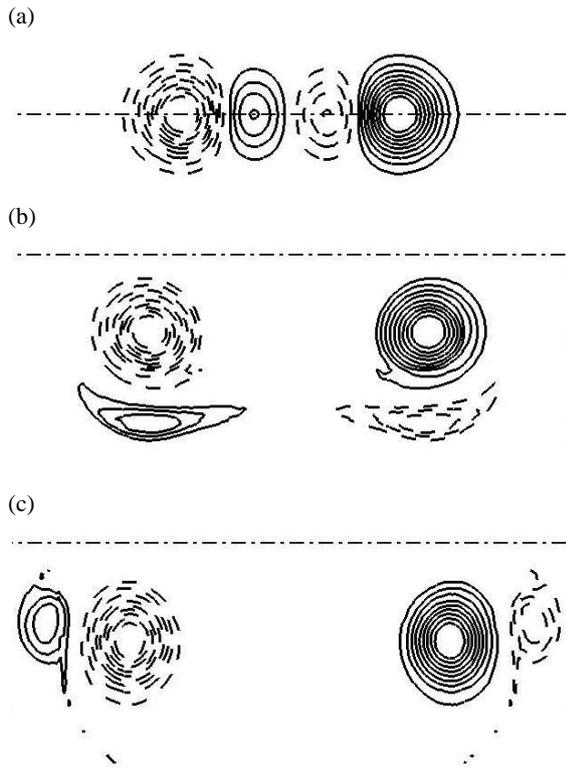
Figure 5: Contour plot of the vorticity of the flat tail case in two-dimensional space at **(a)** 0, **(b)** 5 and **(c)** 10 time units. Each contour line represents a vorticity scale of 0.5. Minimum vorticity is -5.5 with maximum of 5.5 in the left and right wing vortex respectively. Dashed lines represent negative vorticity. Dashed-dot horizontal thin line represents $y = 0$.

(a)

(b)

(c)
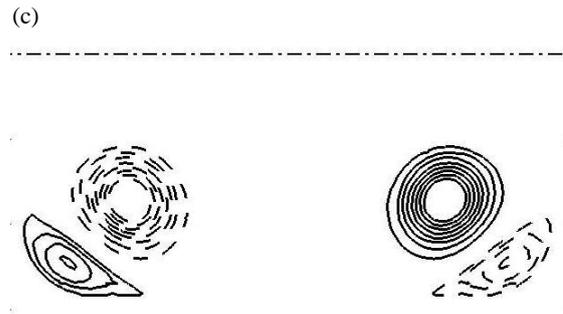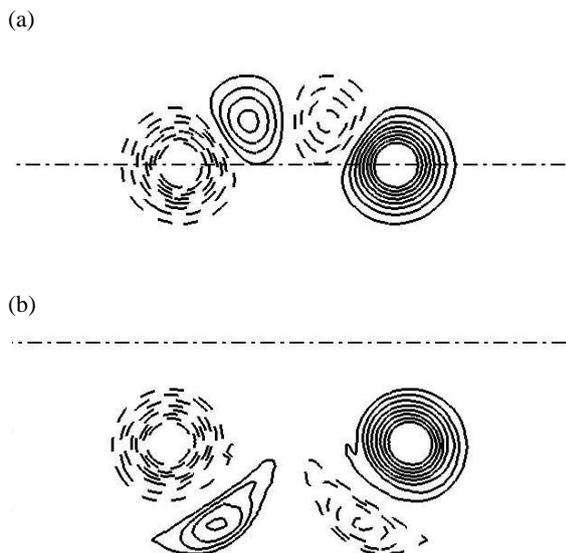
Figure 6: Contour plot of the vorticity of the high tail case in two-dimensional space at **(a)** 0, **(b)** 5 and **(c)** 10 time units. Contour scale, min/max vorticity and dashed and dash-dot lines are as Figure 5.

(a)

(b)
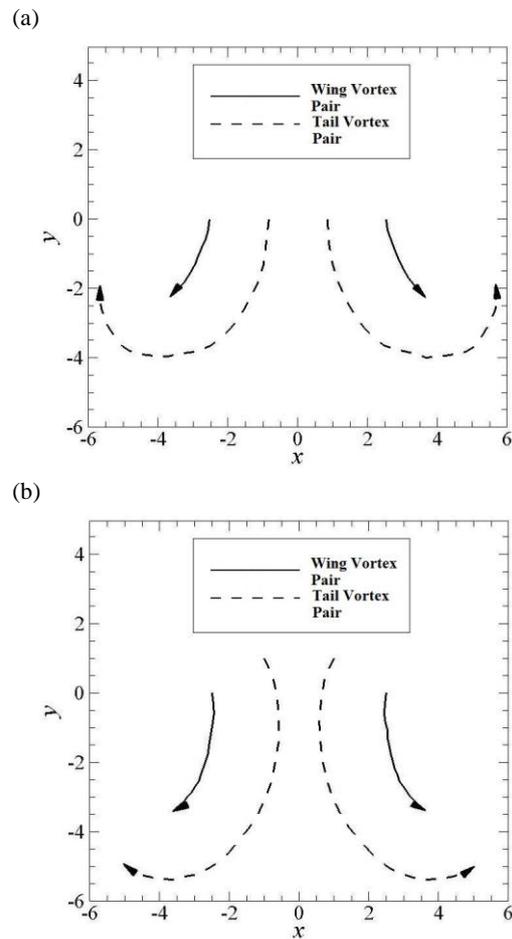
Figure 7: (a) Two-dimensional cartesian plot of the movement of the vortex set in a 'flat tail' configuration. **(b)** Two-dimensional cartesian plot of the movement of the vortex set in a 'High tail' configuration The dashed lines represent the trajectory of the tail vortex pair and the solid lines represent the trajectory of the wing vortex pair. The two inner arrows display the movement of the smaller tail vortex pair. The arrowhead represents the position after 10 time units. No cross flow was imposed on the short term simulation to allow for absolute trajectories to be observed.

It can be seen in Figure 7(b) that an initial vertical displacement of the tail vortex pair by as little as $0.2b_1$ causes the wing vortex pair to descend to approximately $0.76b_1$ over the initial 10 time units.

This is due to the tail vortex pair providing a downward driving force for longer timeframe in the initial stages before it swings beneath the wing vortex pair. After 10 time units, the displacement for the 'high tail' is almost double the 'flat tail' case. This would contribute significantly to pushing the wing vortex pair out of the flight path of trailing aircraft.

Vortex circulation history

It can be seen in figure 8 that the general trend for the circulation of the tail is very similar for both the 'high tail' and 'flat tail' case. It is important to note, however, that the 'high tail' case begins with approximately 20% more circulation than the 'flat tail' case.
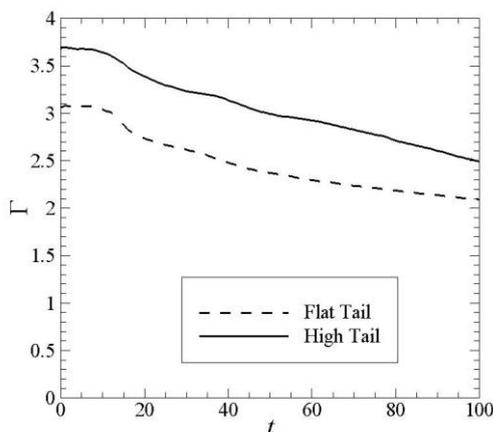
Figure 8: Plot of the circulation of the positive tail vortex. The dashed line represents the circulation for the flat tail case and the solid line represents the high tail case.

This is most likely due to the tail vortex pair in the 'flat tail' case having a reduced area due to its extremity overlapping with the stronger wing vortex pair. The 'high tail' case has more room to form and as such covers a larger area, with less overlap with the wing vortex pair.

The increased circulation in the 'high tail' case will induce greater vorticity and this will have several effects. As the tail vortex pair has more circulation in the 'high tail' case, then the tail vortex pair will take longer to viscously diffuse. This will cause the main wing vortex pair to vibrate for longer as the tail vortex pair spins around them. This vibration will likely lead to greater instability in the main wing vortex pair and could lead to faster breakdown.

Two dimensional instabilities

It can be seen that the high tail case has a significant effect on the time it takes for a two-dimensional instability to form and grow within the weaker tail vortex pair.

(a)
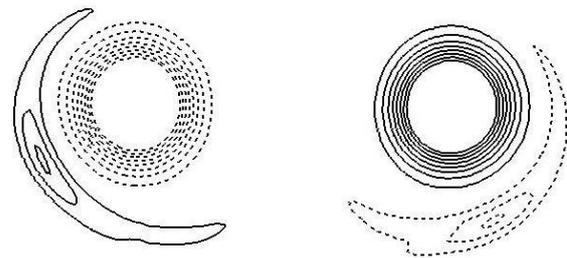
(b)
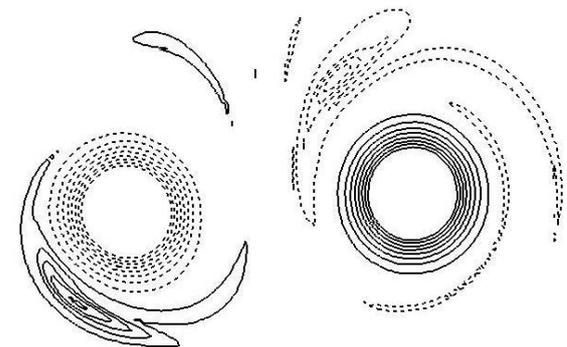
Figure 9: **(a)** Contour plot of vorticity at 100 time units for the flat tail case in two-dimensional space. **(b)** Contour plot of vorticity at 100 time units for the high tail case in two-dimensional space. Each contour line representing a vorticity scale of 0.2. Minimum vorticity is -3.99 with a maximum of 3.99 in the left and right wing vortex respectively.

Figure 9(a) shows that the two dimensional instability is only just beginning to form in the 'flat tail' case after 100 time units as the two tail vorticies lose symmetry about the centerline.

Figure 9(b) shows that the instability is significantly more pronounced at 100 time units for the 'high tail' case. This instability is beginning to have an effect on the position of the wing vortex pair. This effect causes the wing vortex pair to rotate about the centerline and causes the system to become severely unbalanced. The initial onset of this instability for the 'high tail' case is around 75 time units, so the vertical displacement of the tail vortex pair has a significant effect on the time that this instability develops.

Figure 10 shows the plot of the u-velocity recorded at a point (0,0) and shows how the flow is cyclically disturbed in phase with the passage of the tail vortex pair between the wing vortex pair. This period is approximately 20 time units and shows how in the flat tail case, the instability slowly grows. In the high tail case, however, the u-velocity becomes highly perturbed beyond approximately 75 time units.
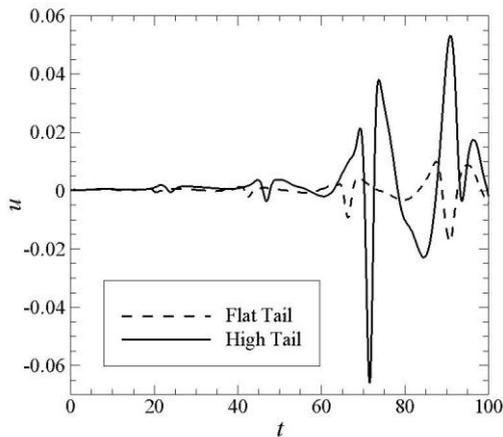
Figure 10: Plot of velocity in the *x*-direction against time for the position (0,0). The solid line represents the velocity for the high tail case and the dashed line represents the flat tail case.

CONCLUSION

The results presented and discussed in this paper clearly show that the vertical displacement of the tail vortex pair has a significant effect on the kinematics, the circulations and the instabilities present in the four-vortex system in two-dimensions.

The 'high tail' configuration has the kinematic effect of initially driving the wing vortex pair vertically downward almost double the distance than the 'flat tail' case.

It was found that due to the increased initial spacing of the vortices, the circulation of the 'high tail' case was approximately 20% higher than the 'flat tail' case. This will cause the tail vortices to take longer to viscously diffuse. The increased life of the tail vortex pair will cause the main wing vortex pair to vibrate for longer due to the viscous forces acting on them. This vibration is likely to induce greater three dimensional instability in the wing vortex pair.

The two-dimensional instabilities present after a long timeframe were found to develop around 75 time units in the 'high tail' configuration while the 'flat tail' did not begin to develop until approximately 100 time units. As this instability causes the system to become unbalanced, this may cause three dimensional instabilities to form faster in the wing vortex pair.

The timeframe of the onset of the two-dimensional instability found in the high tail case is found to be just less than 2 minutes and approximately 7.5 km downstream of a real C-17 aircraft. This instability seems to be localized in the tail vortex pair and doesn't have a large effect on the stability of the wing vortex pair.

This work highlights just how significant a small change in vertical displacement of the tail vortex pair can be in the dynamics of the entire wake system. The standard 'flat tail' configuration that has been investigated in the past does not seem to exhibit the two dimensional

instability that the 'high tail' configuration develops. This is significant as it would not be predicted by a point vortex model and this symmetry breaking instability leads to a non-symmetrical vibration in the wing vortex pair. This non-symmetrical vibration is likely to lead to faster onset of three-dimensional instability. This could lead to breakdown of the vortex system faster in a 'high tail' configuration than in the 'flat tail' configuration.

Future work will focus on the two-dimensional instabilities and the relationship of the time of the onset of the instability and the change in *h*. In addition, future work will extend to three dimensional simulations to observe the effect of the 'high tail' on three-dimensional instabilities.

REFERENCES

BARKER, S.J. and CROW, S.C., (1977), "The motion of two-dimensional vortex pairs in a ground effect, Journal of Fluid Mechanics", *J. Fluid Mech.,* **82**, 659-671.

CROUCH, J.D., (1997), "Instability and transient growth for two trailing-vortex pairs", *J. Fluid Mech.,* **350**, 311-330.

DONALDSON, C. and BILANIN, A., (1997), "Vortex wakes of conventional aircraft", *Tech. Rep.*, AG-204. AGARD.

FABRE, D., JACQUIN, L. and LOOF, A., (2002), "Optimal perturbations in a four-vortex aircraft wake in counter-rotating configuration", *J. Fluid Mech.,* **451**, 391-328.

KARNIADAKIS, G.E., ISRAELI, M., ORSZAG, S.A., (1991), "High-Order splitting methods for the Incompressible Navier-Stokes Equations", *J. Comp. Phys.*, 97, 414-443.

MCCORMICK, B.W., (1995), "Aerodynamics, Aeronautics and Flight Mechanics, 2nd Edition", *John Wiley & sons, Inc., 110-112.*

RENNICH, S.C. and LELE, S.K., (1999), "A method for accelerating the destruction of aircraft wake vortices", *J. Aircraft*, **36**, 398-404.

ROY, C., SCHAEFFER, N., LE DIZES, S., and THOMPSON, M., (2008), "Stability of a pair of co-rotating vortices with axial flow", *Phys. Fluids,* **20**, article number 094101.

SHEARD, G.J., LEWEKE, T., THOMPSON, M.C. and HOURIGAN K, (2007), "Flow around an impulsively arrested circular cylinder", *Phys. Fluids*, **19**(8), article number 083601.